Earth and Planetary Science Letters 284 (2009) 44–49

Contents lists available at ScienceDirect

Earth and Planetary Science Letters

journal homepage: www.elsevier.com/locate/epsl

Broad, weak regions of the Nankai Megathrust and implications for shallow coseismic slip

N.L.B. Bangs [a,*], G.F. Moore [b,c], S.P.S. Gulick [a], E.M. Pangborn [a], H.J. Tobin [d], S. Kuramoto [c], A. Taira [c]

[a] University of Texas Institute for Geophysics, J.J. Pickle Research Campus, Bldg. 196; 10100 Burnet Road (R2200); Austin TX 78758-4445, United States
[b] Dept. Geology and Geophysics, University of Hawaii, Honolulu, HI 96822, United States
[c] Center for Deep Earth Exploration (CDEX), Japan Agency for Marine Earth Science and Technology (JAMSTEC), 3173-25 Showa-machi Kanazawa-ku, Yokohama Kanagawa 236-0001, Japan
[d] Dept. of Geology and Geophysics, University of Wisconsin, Madison WI 53706, United States

ARTICLE INFO

Article history:
Received 15 October 2008
Received in revised form 3 April 2009
Accepted 7 April 2009
Available online 4 June 2009
Editor: R.D. van der Hilst

Keywords:
splay fault
subduction zone megathrust
seismogenic zone
3D seismic imaging

ABSTRACT

Deep within the Nankai Trough subduction zone the plate-boundary thrust slips along a well-imaged megasplay fault system during the megathrust earthquakes that regularly strike southwest Japan. The routing of the active plate-boundary thrust along an upward-branching splay fault causes deep underthrusting of an unusually thick section of material attached to the subducting ocean crust. Here we present three-dimensional seismic reflection data that shows this unusually thick section is fluid-rich sediment that results in broad, weakly-coupled regions of the megathrust down into the updip end of the seismogenic zone. The weakly coupled regions lie above an underthrust low seismic impedance (presumed to be low-velocity and low-density) sediment section that is between one and two kilometers thick and covers ~3300 km^2, at least one-eighth of the total rupture area of the 1944 Mw 8.1 Tonankai earthquake. This underthrust sediment section is broader and much deeper than inferred at other margins. Sediment underthrusting into the normally well-coupled seismogenic zone likely releases fluids and elevates fluid pressure, which reduces inter-plate coupling along portions of the megasplay fault and allows coseismic rupture to propagate to unusually shallow depths and generate large tsunami as inferred for the 1944 Tonankai event. Splay faults may be a common, yet transient mechanism for developing weak subduction zone thrusts.

1. Introduction

Recent investigations by Park et al. (2002) discovered the megasplay fault system along the Nankai Trough subduction zone beneath the Kumano forearc basin and Nankai Trough accretionary wedge (Fig. 1). The megasplay fault branches upward from the plate-boundary detachment near the top of the subducting crust at ~10–11 km subseafloor, and cuts up more than 2–3 km into the overriding plate before branching again into several splays that intersect and deform the accretionary wedge, as interpreted from regional 2-D seismic lines and the new 3D data volume shown in Fig. 1 (Moore et al., 2007). Regional 2-D seismic lines also constrain the lateral, along strike extent of the splay fault system as 50 km to the NE and 38 km to the SW of the 3D survey for a total of ~100 km width (Park et al., 2003).

The megasplay fault is believed to branch upward from the plate boundary within rocks with temperatures greater than 200 °C (Park et al., 2002), much hotter than the inferred aseismic-to-seismic transition at ~150 °C (Moore and Saffer, 2001). Thus slip along the deeper segments of the megasplay fault may be within the seismogenic zone and contribute to the devastating large subduction zone megathrust earthquakes recorded along this margin (Kikuchi et al., 2003; Fig. 1). Park et al. (2002) showed that this thrust is a major slip surface that accommodates strain between the subducting and overriding plates. Its geometry runs directly through the accretionary wedge and forms an out-of-sequence thrust, probably directing slip to the seafloor at the upper slope, rather than seaward along the décollement beneath the lower slope (Moore et al., 2007; Fig. 1). The most recent Mw 8.1 Tonankai event in 1944 produced a tsunami probably due to slip along the splay fault (Moore et al., 2007; Baba and Cummins, 2005). In this paper we present new 3D seismic reflection data to examine the reflection characteristics of deep splay fault system to infer mechanisms of deep sediment subduction and implications for shallow coseismic slip.

2. New 3D seismic reflection data across the Nankai subduction zone

2.1. The deep megasplay fault system and deep sediment underthrusting

In April 2006, we acquired a new 3-D seismic reflection data volume to map the detailed structure of this thrust system. We accurately imaged the high-amplitude seismic reflection produced by

* Corresponding author. University of Texas-Institute for Geophysics, 10100 Burnet Rd., PRC 196, Austin, TX 78758, United States. Tel.: +1 512 471 0424; fax: +1 512 471 0348.
E-mail address: nathan@ig.utexas.edu (N.L.B. Bangs).

0012-821X/$ – see front matter © 2009 Elsevier B.V. All rights reserved.
doi:10.1016/j.epsl.2009.04.026

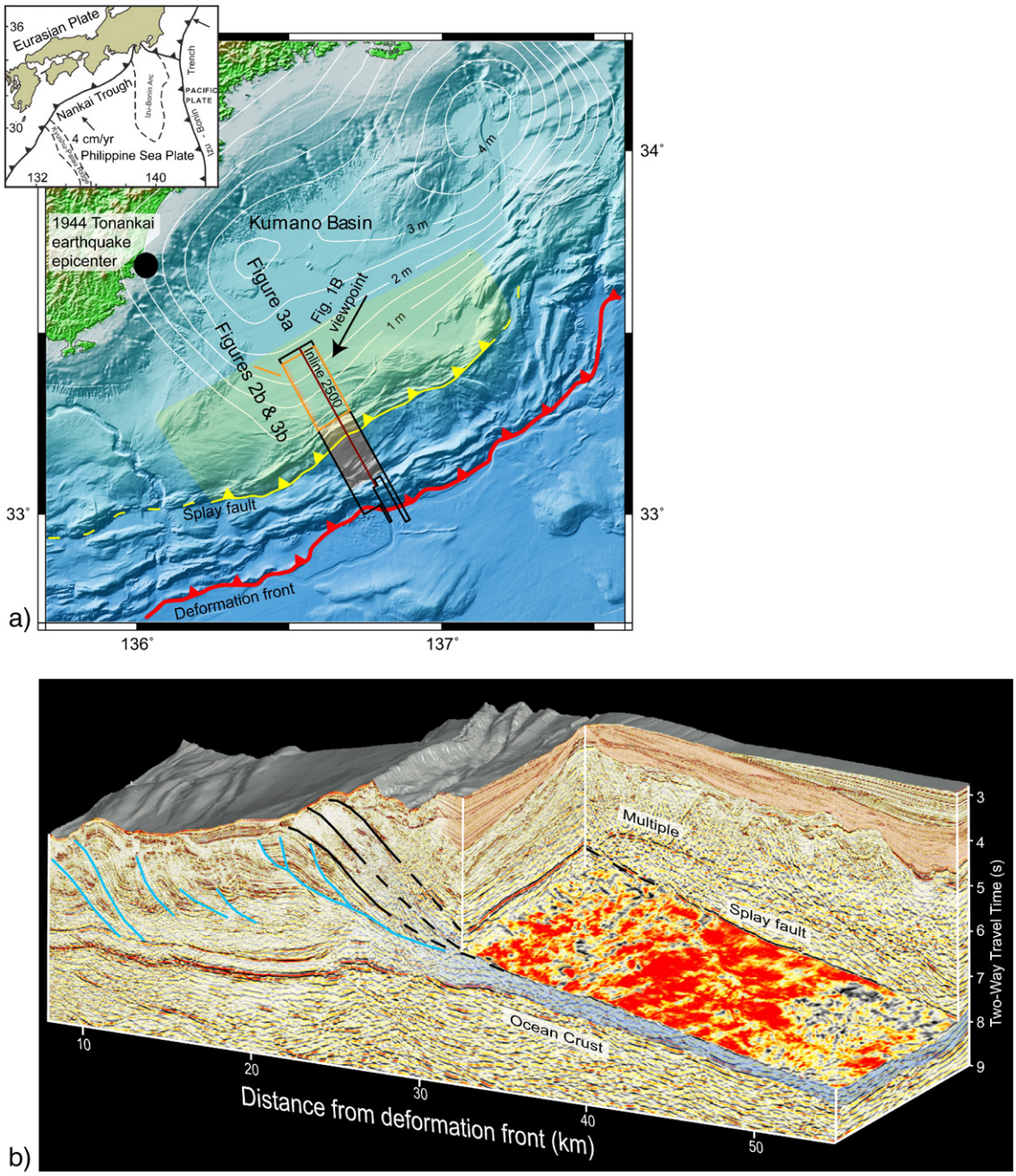

Fig. 1. a) Location map of the Kumano Basin 3D seismic reflection survey. The survey dimensions are 12 × 50 km covering the outer accretionary wedge into the Kumano forearc basin (black outline). Gray seafloor is seafloor depicted in Fig. 1b. Brown line is profile shown in Fig. 3a. Orange outline is mapped splay fault shown in Fig. 2b cutout and 3b. White contours show slip during the 1944 M8.1 Tonankai earthquake (Kikuchi et al., 2003). Yellow shading is regional extent of the well-imaged splay fault (Park et al., 2003). b) Perspective view of 3-D seismic volume with cut-out to show high-amplitude, reversed-polarity seismic reflection from the deep splay fault (red areas). Blue shaded area is 1–2 km thick underthrust layer between splay fault and top of the subducting ocean crust, which extend to ~8–10 km sub seafloor on right. Orange shading is uplifted forearc basin sediment horizons, which were uplifted to form the overlying unconformity. Blue lines are accretionary wedge thrusts. Black lines are splay fault branches (Moore et al., 2007). The inferred underthrust section is the interval between these two surfaces. Note the tilted strata of the Kumano forearc basin along its seaward margin.

the deep megasplay fault to infer the physical properties of this fault and interpret its role in the seismogenic zone and subduction zone processes. Our images of the megasplay fault within the 3D seismic data show a high-amplitude seismic reflection that is present from the seafloor at the seaward edge of the Kumano basin to 8 s (8 – 10 km sub seafloor) (Fig. 1b). Surprisingly there is a 1–2 km thick zone of sediment beneath the entire 25 km extent of the megasplay fault in the down-dip direction that extends across the 12 km width of our seismic survey. We infer that it is this underconsolidated, underthrust material that gives rise to the high amplitude of the megasplay fault reflection. This underthrusting has introduced a massive volume of potentially weak, fluid-rich material into the up-dip end of seismogenic zone permitting ruptures to likely propagate up-dip to unusually shallow depths along the megasplay fault.

Previous studies characterized the megasplay fault reflection as polarity reversed relative to the seafloor, implying a decrease in impedance (the product of velocity and density) at the interface (Park et al., 2002). What remained unclear from the older 2-D data were the detailed waveforms of the megasplay reflection and their regional characteristics. The waveforms are now sharp due to our well-tuned source array, minimal noise, and 3D processing, and reveal the broad nature of this fault zone boundary (see Moore et al., 2009 for more

details about the 3D data). Plate boundary fault zones have been shown to be low-velocity, fluid-rich, underconsolidated thin (10s of m) layers along some margins (e.g. Bangs et al., 1999; Moore et al., 1998), and at other margins they can be boundaries that juxtapose underconsolidated, underthrust sections beneath older, consolidated rocks creating the contrast across the fault zone (Moore et al., 2001). Our new 3D data imaged this fault with sufficient detail to reveal the reflective properties across a broad area of the megasplay fault, and highlight the role of the underlying sediment properties in creating the fault-plane reflection.

2.2. Waveform characteristics

A primary goal with our new 3D images is to accurately assess waveform characteristics across the megasplay fault at depth to reveal regional fault properties and determine the nature of the deep extension of the splay fault. We investigate how assumed fault structure affects reflection waveform symmetry and amplitude (Widess, 1973; Zeng and Backus, 2005). Fig. 2a (left) shows the typical megasplay fault-plane reflection waveform (mostly asymmetric) and three models that include A) a low-impedance layer sufficiently thin to cause reflection interference at the layer interfaces (i.e., tuning; Widess, 1973) (nearly symmetric waveform), B) a decrease in impedance at a single interface (nearly asymmetric waveform), and C) a similar interface with a minor increase in impedance within a thin, tuned layer above the low-impedance boundary (nearly asymmetric). On the basis of symmetry and amplitude of the waveform lobes, the poorest waveform match to the data is the thin layer (A in Fig. 2a). Models B and C are both close to the observed waveform. The amplitude effect on waveform from thin, low-impedance layer tuning is an increase of the trough amplitude of up to twice the peak amplitude for a 90°-phase wavelet (Zeng and Backus, 2005) (for a minimum phase wavelet, such as ours, the result is nearly identical). Therefore, the trough amplitude relative to the peak is sensitive to the tuning effect as illustrated in Fig. 2a. Peak-to-trough ratios from the reflection waveform are easily derived from the megasplay fault-plane reflection and are a convenient way to map waveform characteristics over the broad 3D coverage area. Fig. 2b includes only peak-to-trough ratios of high-amplitude reflections that are well above noise level and covers only ~40% of the fault area. Other areas (dark gray in Fig. 2b) show similar results but with higher uncertainty due to lower reflection strength relative to noise. Ratios are broadly consistent with the example reflection shown in Fig. 2a (i.e., >0.8) and well above what is expected for a thin layer, 0.5. Little or no tuning effect is detected.

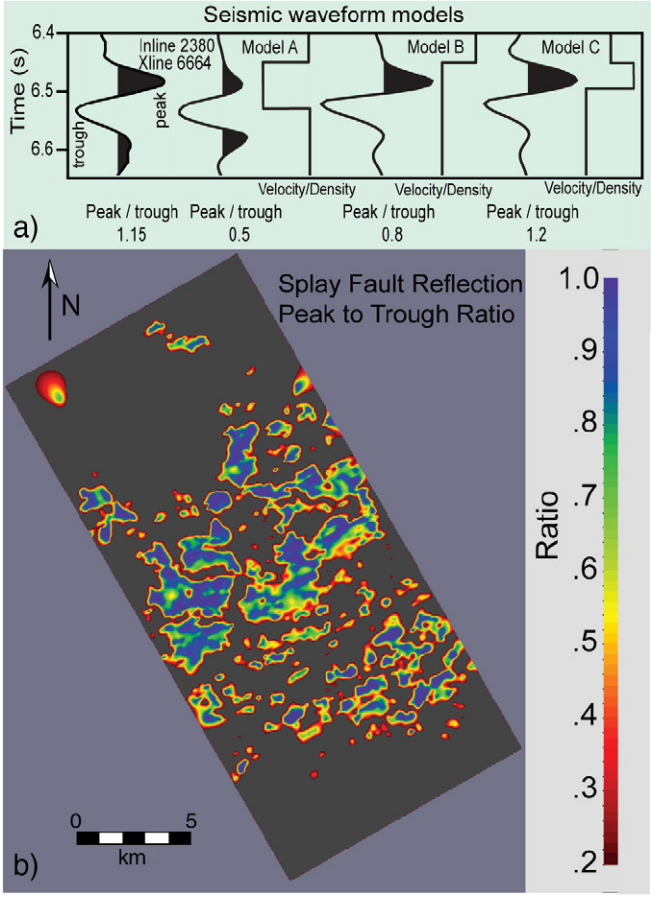

Fig. 2. a) The deep splay fault reflection seismic waveform and possible models depicted with relative velocity and density changes. Each of the models produces a distinctive waveform with a characteristic peak to trough ratio. Models B and C are a closer match to the splay fault reflection waveform (left). b) The splay fault reflection peak-to-trough ratio (in percent) extracted only from the largest amplitude reflections. Note the ratio is consistently above .7 (green to blue), consistent with models B and C (Fig. 1a) and rarely near .5 (orange to light red), which would indicate model A. The dark gray areas show similar results but have greater uncertainty due to weak signal relative to noise.

On the basis of our modeling, we interpret the megasplay fault-plane reflection as an interface caused by a step down into lower-velocity and lower-density sediment, with some possibility of a thin higher-velocity, higher-density layer immediately above this interface (i.e. Model C). The megasplay fault zone itself may lie within the thin high-velocity, high-density layer, with shearing as the cause of the high impedance. However, the main reflective interface is the result of a contrast in material properties between the overriding and underthrust sections. The typically narrow range of the peak-to-trough ratios implies there is little variation in the reflective pattern of the splay fault across the 3D survey area, thus indicating the reflection from the fault is caused by the broad extent of the underthrust layer and the broad distribution of fluids within that layer.

2.3. An underthrust low-impedance layer

The reflection waveform indicates a low seismic impedance layer, which is commonly caused by a combination of both low-velocity and low-density due to the relationship between porosity and velocity and density (e.g. Erickson and Jarrard, 1998; Hoffman and Tobin, 2004). We attribute the lower impedance to underconsolidated, overpressured sediment beneath the megasplay; however, it does not tell us whether the low-impedance layer extends down to the top of the subducting crust. Analysis of the reflection amplitude from both the splay fault and top of ocean crust indicates the low-impedance material is not confined to a thin interval near the fault zone, but extends throughout the entire interval between the megasplay fault and the ocean crust (Fig. 3, blue shaded interval in Fig. 1).

We see no seismic reflection between the splay fault and the top of the subducting crust that could be the base of the low-velocity, low-density section (Figs. 1b and 3a); however, a non-reflective gradient boundary cannot be ruled out. A clue to the properties of the entire underthrust section is the amplitude at the base of the section, which extends to the top of the subducting ocean crust. Fig. 3 shows the extracted negative polarity reflection amplitude of the megasplay fault and the positive polarity reflection amplitude of the basement reflection over their broad area of overlap. The amplitudes of these reflections correlate with each other to a reasonable degree, especially for the strongest amplitude reflections. To highlight the correlation, we have calculated the ratio of basement to megasplay reflection amplitudes (Fig. 3). Across most of the fault, the basement reflection amplitude is 0.4–0.8 of the megasplay fault reflection amplitude (light blue to yellow in Fig. 3). High-amplitude megasplay fault reflections overlie nearly all of the high-amplitude basement reflections. We interpret the coincident reflection amplitudes as due to low velocity and low density through the entire underthrust section between the megasplay fault and top of subducting basement. We have not yet determined the absolute magnitude through modeling (e.g., Warner

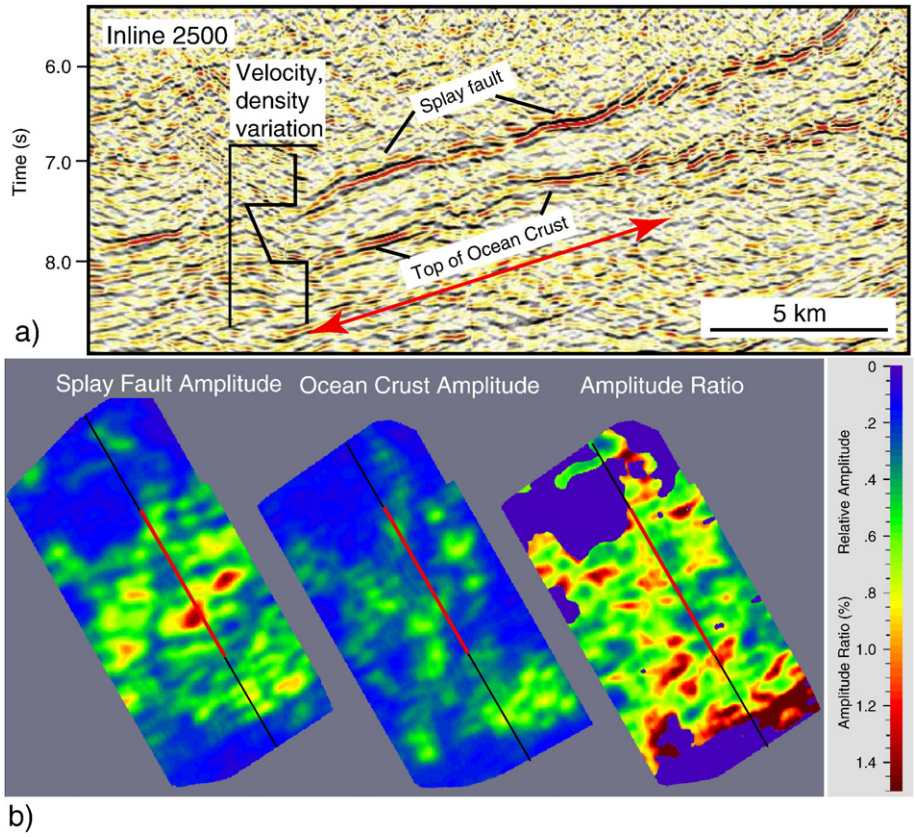

Fig. 3. a) An enlargement of the seismic reflection section showing the deep splay fault and ocean crust reflections down to 8–10 km sub seafloor. Note the high amplitude splay fault reflection directly overlies high amplitude reflections from the top of the subducting crust. The relative velocity/density model shows the inferred variation from the analysis in Fig. 2 and the amplitude of the coincident underlying reflection from the top of ocean crust. The red line marks the corresponding amplitudes shown in this figure. b) Relative amplitude maps from the splay fault (left), top of ocean crust (center) and their ratio in percent (ocean crust/splay) (right). High amplitude splay fault reflections tend to overlie high amplitude ocean crust reflections as indicated by the ratio. The ratio is mostly .4–.6 (green to blue). Ratios greater than .8 tend to be associated with areas of weak and poorly imaged surfaces.

and McGeary, 1987) due to effects on the amplitudes from water column multiple suppression during processing. The multiple suppression does not significantly change the relative amplitudes across the deep splay fault or basement across the section interpreted here, but it does interfere with an absolute calibration of amplitudes. The amplitude ratios do reflect relative changes in reflectivity but currently we can only infer relative property variations as shown in Fig. 3 and we cannot constrain the absolute amounts. We do not believe that data processing has caused other detrimental effects on reflection amplitudes. The only significant effect on reflection amplitude from data processing is a geometric spreading correction, which corrects for depth differences of the megasplay fault and ocean crust reflections and allows comparison of relative amplitudes independent of their depth.

The relative impedance changes across the deep megasplay fault and the top of ocean crust are intriguing and can be explained by a broad low-velocity, low-density layer between these two interfaces. The correlation between these reflections implies that the anomalous low-velocity, low-density within the underthrust layer is affecting the impedance contrasts at both interfaces. An increase in velocity and density with depth along a smooth gradient within this section could reduce the impedance contrast at the top of the ocean crust and reduce the reflection amplitude relative to the megasplay fault reflection as we observe, but velocity and density remain relatively low within the entire underthrust interval to produce a reflection from the top of ocean crust that has an amplitude that is 40%–80% of the megasplay fault reflection. The seismic velocity information that we can derive directly from the seismic reflection data has poor velocity resolution at this depth due to the short (4500 m) source receiver offsets and thus it is insufficient to detect velocity inversions such as inferred in Fig. 3, but still adequate for approximate time-to-depth conversion. No existing refraction surveys are of adequate resolution to detect this anomalous layer.

2.4. Correlation between sediment underthrusting and Kumano Basin uplift

Directly overlying the underthrust section described here are tilted strata of the Kumano forearc basin (Fig. 1b). The tilted strata were also noted by Park et al. (2002) and form a regionally significant 100-km-long “outer ridge” along the seaward edge of the Kumano Basin. The tilted strata and outer ridge extend along strike across the entire Kumano area, including the area imaged by the 3D volume, and lie directly above the megasplay fault. The strata record uplift of the seaward edge of the Kumano Basin as inferred by the stratal reorientation and resulting unconformity (Fig. 1b). We note that the thickness of the underthrust section is closely equivalent to the inferred uplift of these strata as interpreted from the stratigraphy of the Kumano Basin, suggesting a striking correlation between the geometry of the low-impedance layer, and the uplifted forearc basin strata. This correlation suggests that the thrusting along the megasplay fault resulted in underthrusting of sediments as well as uplift of the seaward edge of the Kumano forearc basin.

3. Discussion

We interpret the low-impedance layer beneath the megasplay as low-velocity, low-density sediments that are underconsolidated due to delayed consolidation following underthrusting beneath the rigid overriding crust underneath the Kumano forearc basin (Fig. 4). It is

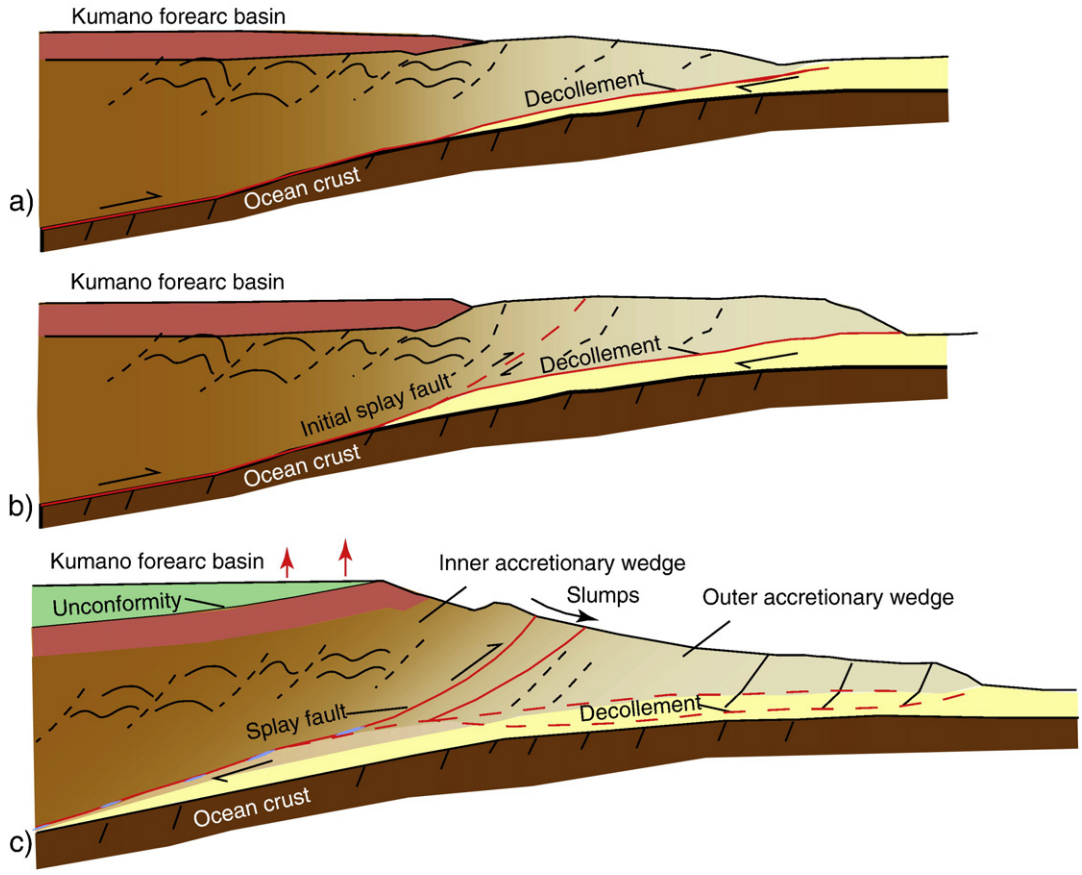

Fig. 4. Models of the initiation of the splay fault and development of the underthrust section. This is an approximate model to illustrate the relationship between the underthrust sediment and the uplift of the seaward edge of the Kumano Basin following the development of the splay fault. Planned future work as part of the NanTroSEIZE project will provide further constraints for this preliminary model. a) prior to splay fault initiation sediment accumulates in the forearc basin and sediment is accreted into the outer accretionary wedge. Shallowing of the décollement may lead to splay fault development as shown in (b). b) The splay fault initiates, causing slip to bypass the primary slip surface (décollement) beneath the outer accretionary wedge and begin to underthrust outer wedge sediment beneath the Kumano Basin. c) With continued thrusting along the splay fault, a thick underthrust section of low-impedance (presumed to be low-velocity and low-density) outer wedge sediment is underthrust beneath the Kumano Basin causing uplift and tilted forearc basin strata. Slumping and shortening thickens the outer wedge, and the décollement steps down into the underthrust section to its current location. Fluids from the underthrust section may migrate into the fault zone (blue patches) and maintain high pore fluid pressures that enable coseismic slip.

not possible for this 1–2 km thick low-velocity, low-density layer to develop in situ by dilation following injection of fluids migrating into this interval from deep sources or from fluid production, because these underthrust sediments are much deeper (and at higher temperatures) than major fluid production sources that are limited to the shallowest 4–5 km (Moore and Saffer, 2001). Similar high-amplitude reflections at the base of the overriding plate within the Costa Rica margin have been attributed to fluid production from mineral dehydration reactions (Ranero et al., 2008). Fluid production there generates an increase in the plate-boundary reflection amplitude with depth until fluid production ceases at ~150 °C. In our survey region the reflection maintains a high reflection amplitude that can be traced all along the deep megasplay to depths much greater than expected for fluid production and don't appear to build up to a maximum at ~150 °C. We believe that pore fluid and fluids produced from dehydration reactions are delayed in escaping from the underthrust layer, similar to that found within an underthrust sediment layer of similar thickness beneath the Peru margin by Calahorrano et al. (2008). In their example, however, there is an abrupt transition to substantially lower water content in the underthrust layer between depths of 4.0–4.5 km below seafloor. Their example illustrates the unusually great depth of the underthrust sediment layer in the Kumano Basin region.

Underconsolidated materials with sufficient porosity to produce the bright reflections are particularly anomalous below 5 km sub seafloor and are inferred to have been recently thrust beneath the Kumano Basin by slip on the splay fault. Because the megasplay fault extends directly through the inner wedge to the seafloor, slip along this fault causes shallow sediment with low-velocity and low-density to be thrust directly under the Kumano Basin (Fig. 4). Some of these sediments are probably previously accreted sediment that is then eroded following the development of the splay fault; however, this depends on the past position and displacement of the décollement thrust and we have no constraint on this. This mechanism temporarily or intermittently bypasses a more typical longer path along the outer wedge décollement, and bypasses the typical sediment compaction or underplating processes that allow only small amounts of highly compacted sediment subducted into the seismogenic zone. Regional 2-D seismic lines show that the splay fault extends 100 km along strike implying an underthrust volume covering an area 33 x 100 km^2. This section is similar to patches observed along other margins (e.g. Sage et al., 2006; Calahorrano et al., 2008) but here the underthrust volume is larger, it creates a broader zone of weak coupling than has been previously inferred, and it can be seen to extend to much greater depths.

Previous studies of fault reflectivity show either localized, km-sized underconsolidated zones within the shallow to intermediate plate-boundary fault (Shipley et al., 1994, Ranero et al. 2008) or broad zones of underconsolidated, underthrust sediment that compact near the toe of the accretionary wedge and nearly eliminate the seismic reflection before underthrusting deeper than ~3–4 km sub seafloor (Bangs et al., 2004; Calahorrano et al., 2008). Beneath the Kumano

Basin broad areas of underthrust sediment extend to >10 km below seafloor, much deeper than seen previously. This observation raises significant issues for co-seismic rupture due to the potential effect these sediments have on fault behaviour. Porosity is a key factor for the up-dip edge of the seismogenic zone, which typically lies at 4–5 km sub seafloor (Moore and Saffer, 2001). Underconsolidated sediment with anomalously high-porosity thrust as much as 8 to 10 km sub seafloor could significantly deepen the up-dip limit of the seismogenic portion of the megasplay fault. Weak high-porosity materials thrust deep into the seismogenic zone would tend to behave as they do along the shallow aseismic portions of the thrust. They would lack sufficient competence to lock the fault and sustain large shear stresses; furthermore, they would exhibit velocity-strengthening behaviour that would tend to terminate rupture (Wang and Hu, 2006). Thus, we might expect slip would terminate unusually deep because of the deep sediment underthrusting.

However, from mechanical arguments the megasplay fault is the primary coseismic plate boundary near the up-dip terminus of slip (Kame et al., 2003; Wang and Hu, 2006). The megasplay fault is believed to have recently ruptured to or nearly to the seafloor (Moore et al., 2007) probably during the 1944, Mw 8.1 Tonankai event (Kikuchi et al., 2003; Baba, and Cummins, 2005), which generated a large tsunami. It may also slip episodically in both high-frequency post-seismic events and in much lower frequency "slower" inter-seismic events (Ito and Obara, 2006). These observations imply that the megasplay fault does not accumulate significant inter-plate shear stress that contributes to co-seismic rupture, but can propagate co-seismic rupture. This behaviour may be a direct effect of fluids supplied by the underconsolidated, underthrust section, especially if they are available to elevate pore fluid pressures and thus weaken the overlying fault zone by lowering effective stress (Bangs et al., 2004). The conditions introduced by the sediment underthrusting may lead to an inherently weak plate-boundary fault that does not accumulate significant shear stress but will easily propagate slip initiated farther down dip to anomalously shallow depths. These observations imply a deep locked zone, but shallow coseismic slip. Some coseismic and post seismic slip can still occur along the outer wedge décollement; however, we expect that coseismic slip along the megasplay will propagate up to much shallower depths than coseismic slip that propagates along the outer wedge décollement. Megasplay fault systems seen globally (e.g. Sage et al., 2006), may be a common, possibly transient mechanism for introducing large fluid volumes into the seismogenic zone that can cause shallow up dip propagation of coseismic slip.

Acknowledgments

We thank Kelin Wang, Dave Scholl and César Ranero for their help in improving this manuscript. This project was funded by the National Science Foundation (grant # 0452340), and the Japanese Ministry of Education, Culture, Sports and Technology. This is UTIG contribution #2073.

References

Baba, T., Cummins, P.R., 2005. Contiguous rupture areas of two Nankai Trough earthquakes revealed by high-resolution tsunami waveform inversion. Geophys. Res. Lett. 32, L08305. doi:10.1029/2004GL022320.

Bangs, N.L., Shipley, T.H., Moore, J.C., Moore, G.F., 1999. Fluid accumulation and channeling along the northern Barbados Ridge décollement thrust. J. Geophys. Res. 104, 20,399–20,414.

Bangs, N.L., Shipley, T., Gulick, S., Moore, G., Kuromoto, S., Nakamura, Y., 2004. Evolution of the Nankai Trough décollement from the trench into the seismogenic zone: Inferences from three-dimensional seismic reflection imaging. Geology 32 (4), 273–276.

Calahorrano, A., Sallares, V., Sage, F., Collot, J.Y., Ranero, C.R., 2008. Nonlinear variations of the physical properties along the Southern Ecuador subduction channel: results from depth-migrated seismic data. Earth and Planetary Science Letters 267, 453–467. doi:10.1016/j.epsl.2007.11.061.

Erickson, S.N., Jarrard, R.D., 1998. Velocity-porosity relationships for water-saturated siliciclastic sediments. Journal of Geophysical Research 103 (B12), 30385–30406.

Hoffman, N.W., Tobin, H.J., 2004. An empirical relationship between velocity and porosity for underthrust sediments in the Nankai Trough accretionary prisms. Proc. Ocean Drill. Program Sci. Results 190/196 196SR-355.

Ito, Y., Obara, K., 2006. Very low frequency earthquakes within accretionary prisms are very low stress-drop earthquakes. Geophys. Res. Lett. 33, L09302. doi:10.1029/2006GL025883.

Kame, N., Rice, J.R., Dmowska, R., 2003. Effects of pre-stress state and rupture velocity on dynamic fault branching. J. Geophys. Res. 108, 13–1–13-32 ESE.

Kikuchi, M., Nakamura, M., Yoshikawa, K., 2003. Source rupture processes of the 1944 Tonankai earthquake and the 1945 Mikawa earthquake derived from low-gain seismograms. Earth, Planet. Space 55, 159–172.

Moore, J.C., Saffer, D., 2001. Updip limit of the seismogenic zone beneath the accretionary prism of southwest Japan: an effect of diagenetic to low-grade metamorphic processes and increasing effective stress. Geology 29, 183–196.

Moore, J.C., Klaus, A., Bangs, N.L., Bekins, B., Bucker, C.J., Bruckmann, W., Erickson, S.N., Hansen, O., Horton, T., Ireland, P., Major, C.O., Moore, G.F., Peacock, S., Saito, S., Screaton, E.J., Shimeld, J.W., Stauffer, P.H., Taymaz, T., Teas, P.A., Tokunaga, T., 1998. Consolidation patterns during initiation and evolution of a plate-boundary décollement zone: Northern Barbados accretionary prism. Geology 26, 811–814.

Moore, G.F., Taira, A., Klaus, A., Becker, L., Boeckel, B., Cragg, B.A., Dean, A., Fergusson, C.L., Henry, P., Hirano, S., Hisamitsu, T., Hunze, S., Kastner, M., Maltman, A.J., Morgan, J.K., Murakami, Y., Saffer, D.M., Sanchez-Gomez, M., Screaton, E.J., Smith, D.C., Spivack, A.J., Steurer, J., Tobin, H.J., Ujiie, K., Underwood, M.B., Wilson, M., 2001. New insights into deformation and fluid flow processes in the Nankai Trough Accretionary Prism: results of Ocean Drilling Program Leg 190. Geochemistry Geophysics Geosystem 2 2001GC000166.

Moore, G.F., Bangs, N.L., Taira, A., Kuramoto, S., Pangborn, E., Tobin, H.J., 2007. Three-dimensional splay fault geometry and implications for tsunami generation,. Science 318, 1128–1131.

Moore, G.F., Park, J.O., Bangs, N.L., Gulick, S.P., Tobin, H.J., Nakamura, Y., Sato, S., Tsuji, T., Yoro, T., Tanaka, H., Uraki, S., Kido, Y., Sanada, Y., Kuramoto, S., Taira, A., 2009. In: Kinoshita, M., Tobin, H., Ashi, J., Kimura, G., Lallement, S., Screaton, E.J., Curewitz, D., Masago, H., Moe, K.T., the Expedition, 314/315/316 Scientists (Eds.), Structural and seismic stratigraphic framework of the NanTroSEIZE Stage 1 transect. Proceedings of the Integrated Ocean Drilling Program, vol. 314/315/316, pp. 1–46. doi:10.2204/iodp.proc.314315316.102.2009.

Park, J.O., Tsuru, T., Kodaira, S., Cummins, P.R., Kaneda, Y., 2002. Splay fault branching along the Nankai subduction zone. Science 297, 1157–1160.

Park, J.O., Moore, G.F., Tsuru, T., Kodaira, S., Kaneda, Y., 2003. A subducted oceanic ridge influencing the Nankai megathrust earthquake rupture. Earth Planet. Sci. Lett. 217, 77–84.

Ranero, C.R., Grevemeyer, I., Sahling, H., Barckhausen, U., Hensen, C., Wallmann, K., Weinrebe, W., Vannucchi, P., von Huene, R., McIntosh, K., 2008. Hydrogeological system of erosional convergent margins and its influence on tectonics and interplate seismogenesis. Geochem. Geophys. Geosyst. 9, Q03S04. doi:10.1029/2007GC001679.

Sage, F., Collot, J.Y., Ranero, C.R., 2006. Interplate patchiness and subduction-erosion mechanisms: evidence from depth-migrated seismic images at the central Ecuador convergent margin. Geology 34, 997–1000.

Shipley, T.H., Moore, G.F., Bangs, N.L., Moore, J.C., Stoffa, P.L., 1994. Seismically inferred dilatancy distribution, northern Barbados Ridge décollement: implications for fluid migration and fault strength. Geology 22, 411–414.

Wang, K., Hu, Y., 2006. Accretionary prisms in subduction earthquake cycles: the theory of dynamic Coulomb wedge. J. Geophys. Res. 111, B06410. doi:10.1029/2005JB004094.

Warner, M.R., McGeary, S.E., 1987. Seismic reflection coefficients from mantle fault zones. Royal Astronomical Society Geophysical Journal 89, 223–230.

Widess, M.B., 1973. How thin is a thin bed? Geophysics 38, 1178–1180.

Zeng, H., Backus, M.M., 2005. Interpretive advantages of 90°-phase wavelets: Part 1 — Modeling. Geophysics 70, C7–C15.